Cell Stem Cell, Volume *24*

Supplemental Information

The Mitochondrial Transacylase, Tafazzin, Regulates AML Stemness by Modulating Intracellular Levels of Phospholipids

Ayesh K. Seneviratne, Mingjing Xu, Juan J. Aristizabal Henao, Val A. Fajardo, Zhenyue Hao, Veronique Voisin, G. Wei Xu, Rose Hurren, S. Kim, Neil MacLean, Xiaoming Wang, Marcela Gronda, Danny Jeyaraju, Yulia Jitkova, Troy Ketela, Michael Mullokandov, David Sharon, Geethu Thomas, Raphaël Chouinard-Watkins, James R. Hawley, Caitlin Schafer, Helen Loo Yau, Zaza Khuchua, Ahmed Aman, Rima Al-awar, Atan Gross, Steven M. Claypool, Richard P. Bazinet, Mathieu Lupien, Steven Chan, Daniel D. De Carvalho, Mark D. Minden, Gary D. Bader, Ken D. Stark, Paul LeBlanc, and Aaron D. Schimmer

Figure S1. Related to Figure 1

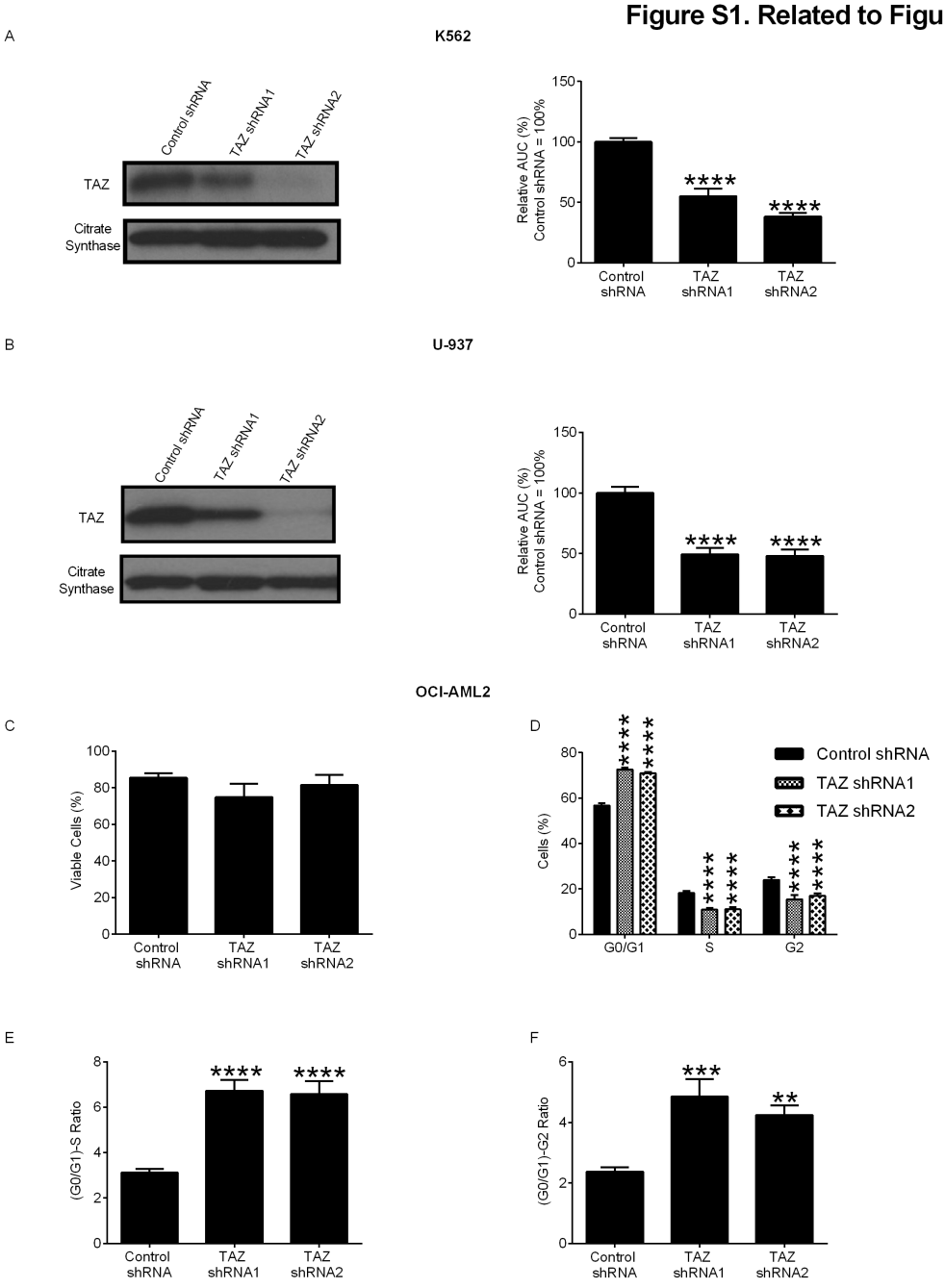

Figure S1. Related to Figure 1. Knockdown of Tafazzin reduces the growth of leukemia cells lines.
(A-B) Proliferation and TAZ protein expression of K562 (A) and U-937 (B) cells after TAZ knockdown. The relative AUC of viable cell counts over 12 days are shown (Control shRNA = 100%). Data are relative mean ± SEM (N = 4, K562; N = 3, U-937, Control shRNA=100%). ****p≤0.0001 using one-way ANOVA and Dunett's post hoc test.
(C) Cell viability of OCI-AML2 cells after TAZ knockdown. Data are mean ± SEM of three independent experiments.
(D-F) Cell cycle status (D) (G0/G1)-S ratio (E), or (G0/G1)-G2 ratio (F), after TAZ knockdown. Data are mean ± SEM of three independent experiments. **p≤0.01, ***p≤0.001, ****p≤0.0001 by Two-Way ANOVA (cell cycle status) or one-way ANOVA (all other graphs) and Dunett's post hoc test.

Figure S2. Related to Figure 2

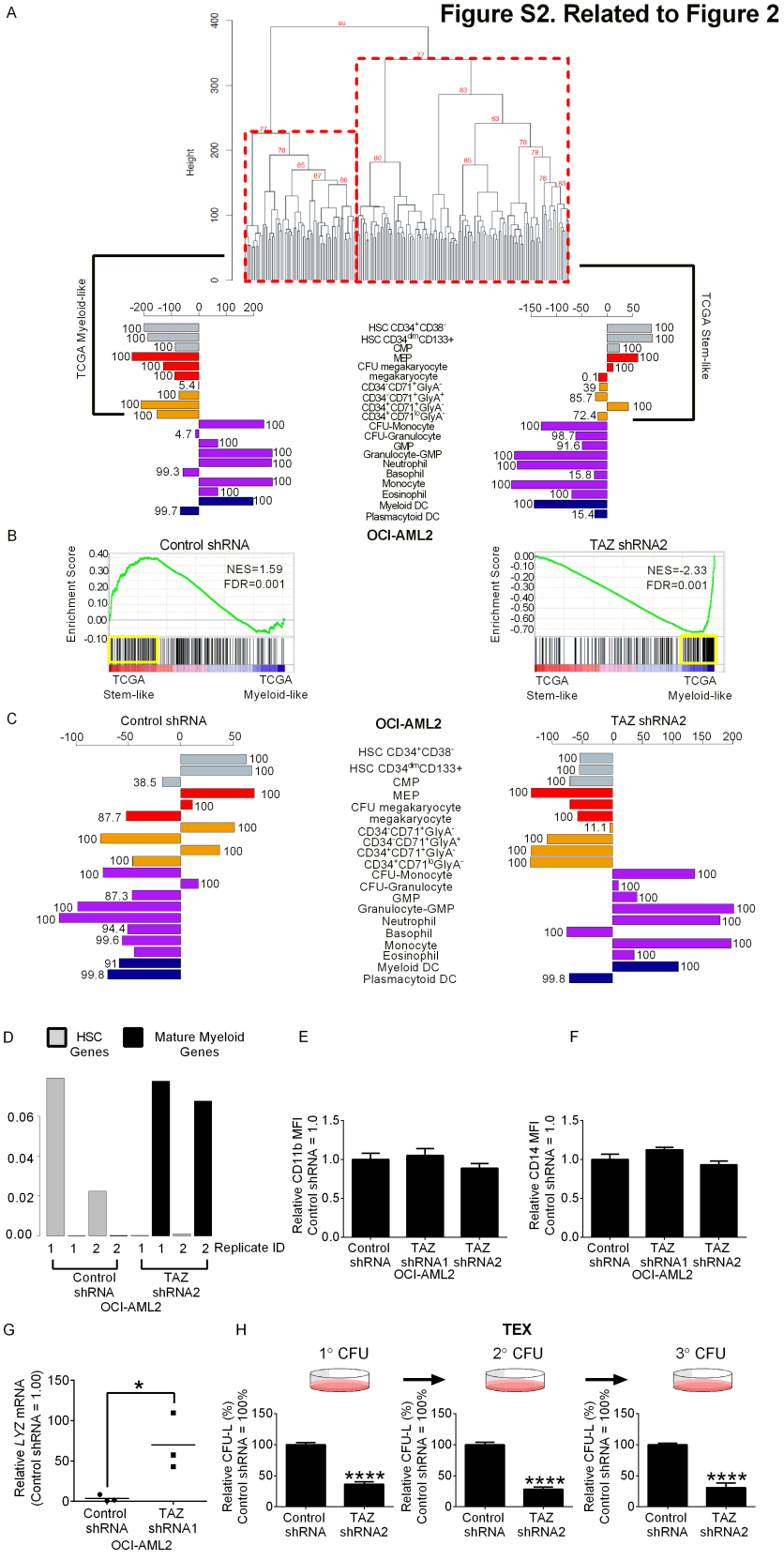

Figure S2. Related to Figure 2. Knockdown of Tafazzin reduces AML Stemness and increases the expression of genes associated with granulocytic/neutrophilic populations.
(A) Unsupervised hierarchical clustering of gene expression data from the TCGA AML cohort (n = 179). Values above each branching represent percent approximate unbiased p values calculated by 1000 boostrap resampling using the R package pvclust. The most differentially expressed genes (top 500) genes between the two TCGA clusters were compared with Gene Expression Omnibus dataset GSE24759 (DMAP) populations. Each bar is a measure of the expression of these genes in each DMAP population compared to the mean of all DMAP populations (mean is equal to 0). Numbers beside bars indicate the percentage of time for which the observed value was better represented in a specific DMAP population than random values (equal number of randomly selected genes based on 1,000 trials).
(B) Gene set enrichment analysis (GSEA) measure of the TCGA stem-like or myeloid-like genes in the TAZ shRNA or control shRNA gene signatures. The normalized enrichment scores (NES), and false discovery rates (FDRs) are indicated in each plot.
(C) The most differentially expressed genes (top 500) between TAZ shRNA2 and control samples were compared with Gene Expression Omnibus dataset GSE24759 (DMAP) populations. Each bar is a measure of the expression of these genes in each DMAP population compared to the mean of all populations (mean is equal to 0). Numbers beside bars indicate the percentage of time for which the observed value was better represented in a specific DMAP than random values (equal number of randomly selected genes based on 1,000 trials).
(D) Proportions of control shRNA or TAZ-KD samples that possess gene expression profiles of undifferentiated HSC or mature myeloid cells, as determined by the perturbation (PERT) deconvolution analysis using gene expression data from normal hematopoietic subsets.
(E-F) CD11b (E) and CD14 (F) expression in OCI-AML2 cells after TAZ knockdown. Data are relative mean fluorescent intensity (MFI) ± SD (n = 3, Control shRNA = 1.0).
(G) Lysozyme (*LYZ*) levels in OCI-AML2 cells transplanted into SCID mice after TAZ knockdown. Data represent relative mean ± SD (n = 3 mice/group, Control shRNA = 1.0). *p≤0.5 by Student's t-test.
(H) Clonogenic growth of TEX cells after TAZ knockdown upon serial replating. Data are relative mean ± SEM of three independent experiments (Control shRNA = 100%). ****p≤0.0001 by Student's t-test.

Figure S3. Related to Figure 3

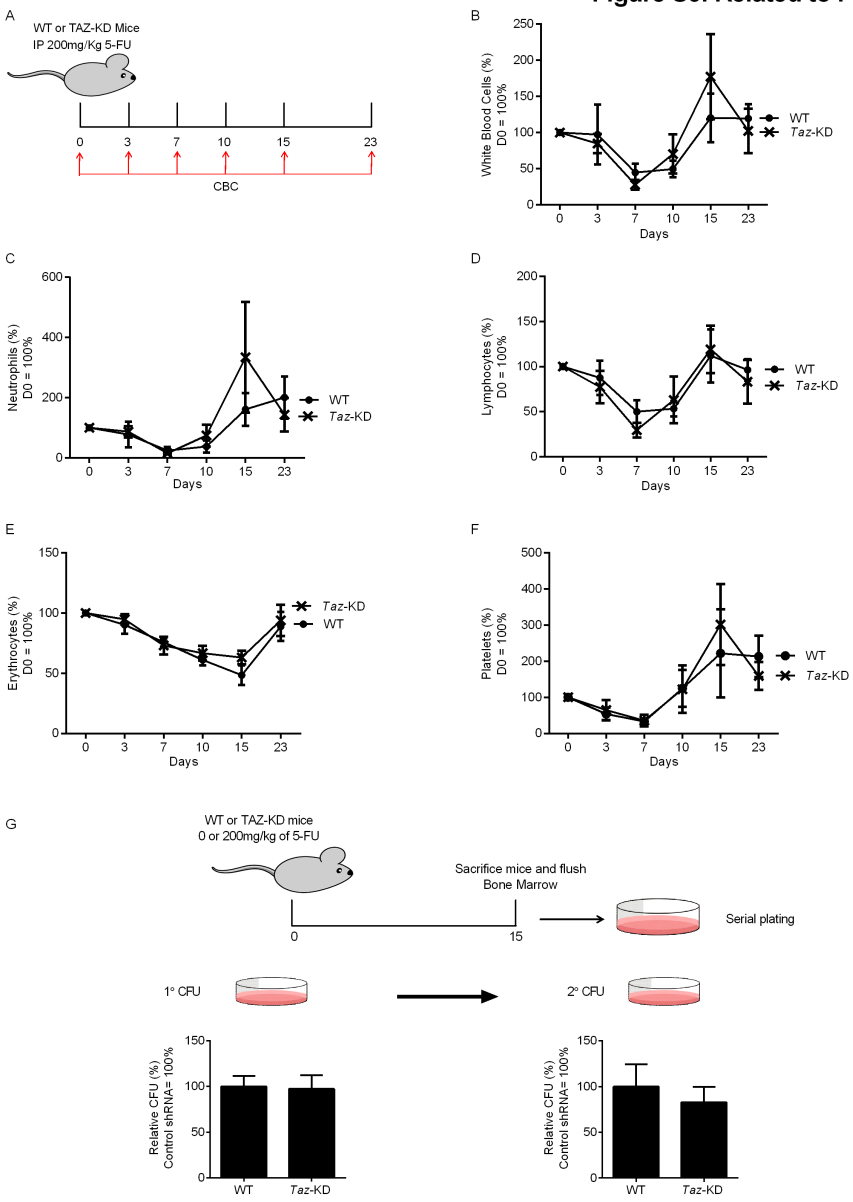

Figure S3. Related to Figure 3. Mature blood counts and progenitor cell function of WT and *Taz*-KD mice after the induction of hematopoietic stress.

(A) Schematic outlining the induction of hematopoietic stress by 5-FU.
WT and *Taz*-KD mice were treated with 200mg/kg of 5-FU i.p. Arrows indicate the days that peripheral blood of WT and TAZ-KD mice were collected.
(B-F) White blood cells (B), neutrophils (C), lymphocytes (D), erythrocytes (E), and platelets (F) levels in the mice in A. Data are relative mean ± SEM of 2 independent mouse groups (n = 7 WT mice, and n = 6 *Taz*-KD mice, D0 = 100%).
(G) Clonogenic growth of hematopoietic cells in 5-FU treated *Taz*-KD mice upon serial replating. Data represent relative mean ± SEM of 2 independent mouse groups (n = 7 WT mice, and n = 5 *Taz*-KD mice, WT mice CFU-GM=100%).

Figure S4. Related to Figure 4

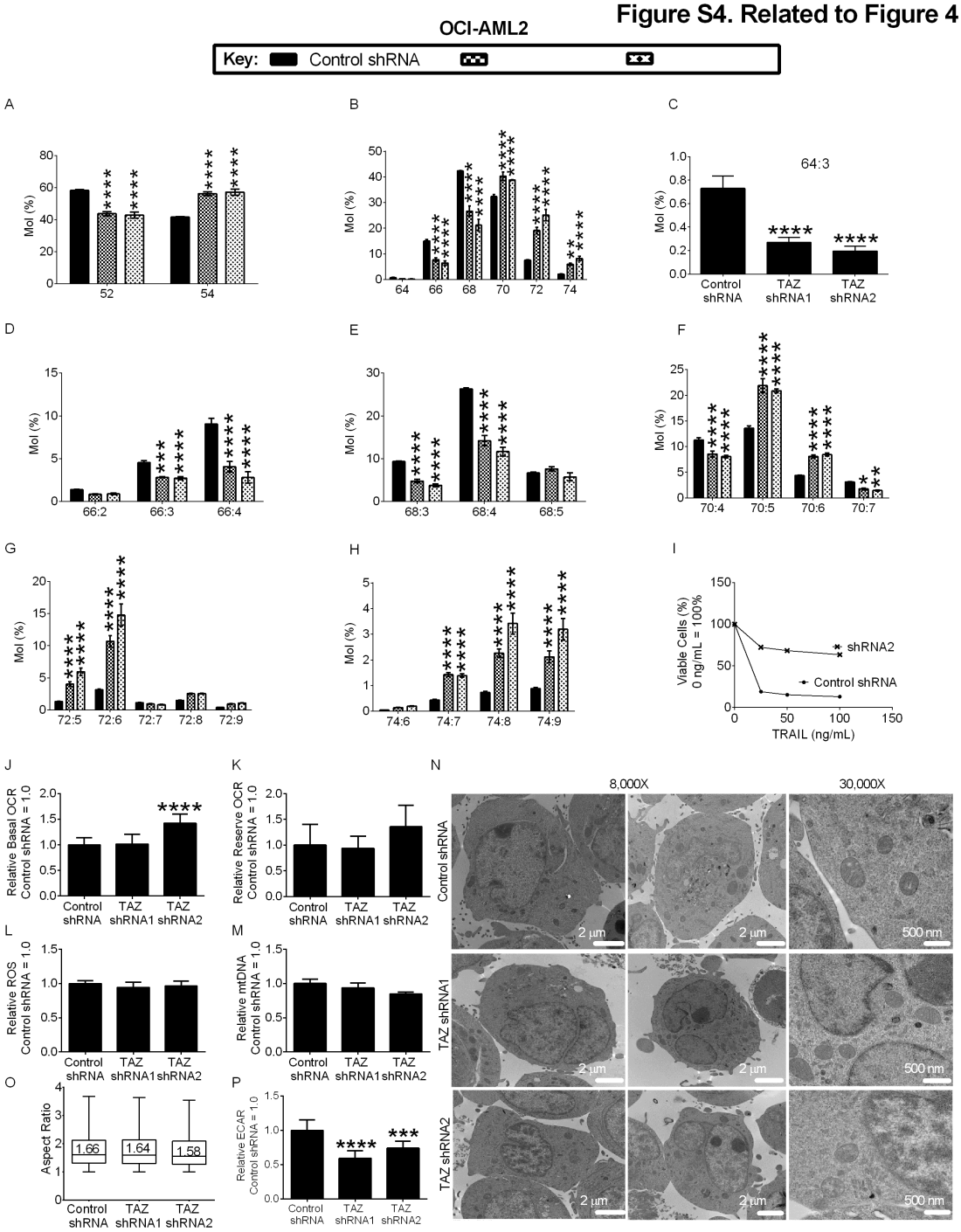

Figure S4 Related to figure 4. Knockdown of Tafazzin in OCI-AML2 cells reduces TAZ activity but does not affect mitochondrial structure or function.

(A-H) The relative abundance of MLCL given chain lengths (A), CL chain lengths (B), and the distribution of double bonds per acyl chain length (C-H). Data are mean ± SEM of three independent experiments. *p≤0.05, **p≤0.01, ***p≤0.001, ****p≤0.0001 by one-way ANOVA (64:3 graph), Two-Way ANOVA (all other graphs), and a post hoc Dunett's test.

(I) Cell viability of OCI-AML2 cell after TAZ knockdown when treated with cyclohexamide, and TRAIL for 16 hours. Data are relative mean ± SD of a representative experiment from 3 independent experiments (0ng/mL TRAIL = 100%).

(J-K) Basal OCR (J) and reserve OCR (K) in OCI-AML2 cells after TAZ knockdown. Data are relative mean ± SD of a representative experiment from 3 independent experiments (Control shRNA=100%). ****p≤0.0001 by one-way ANOVA, and a Dunnett's post hoc test.

(L) Cellular ROS of OCI-AML2 cells after TAZ knockdown. Data are mean ± SD of a representative experiment from 3 independent experiments (Control shRNA = 100%)
(M) Mitochondrial mass of OCI-AML2 cell after TAZ knockdown by the measurement of ND1 levels. Data represent mean ± SD (n=3, Control shRNA = 1.0).
(N) Mitochondrial morphology of cells from D. Composite of representative images are shown. Scale bar = 2μm or 500nM
(O) Boxplot of mitochondrial aspect ratio in OCI-AML2 cells after TAZ knockdown.
(P) ECAR of cells from (A). Data are relative mean ± SD of a representative experiment from 3 independent experiments (Control shRNA=100%). ****p≤0.0001 by one-way ANOVA, and a Dunnett's post hoc test.

Figure S5. Related to Figure 4

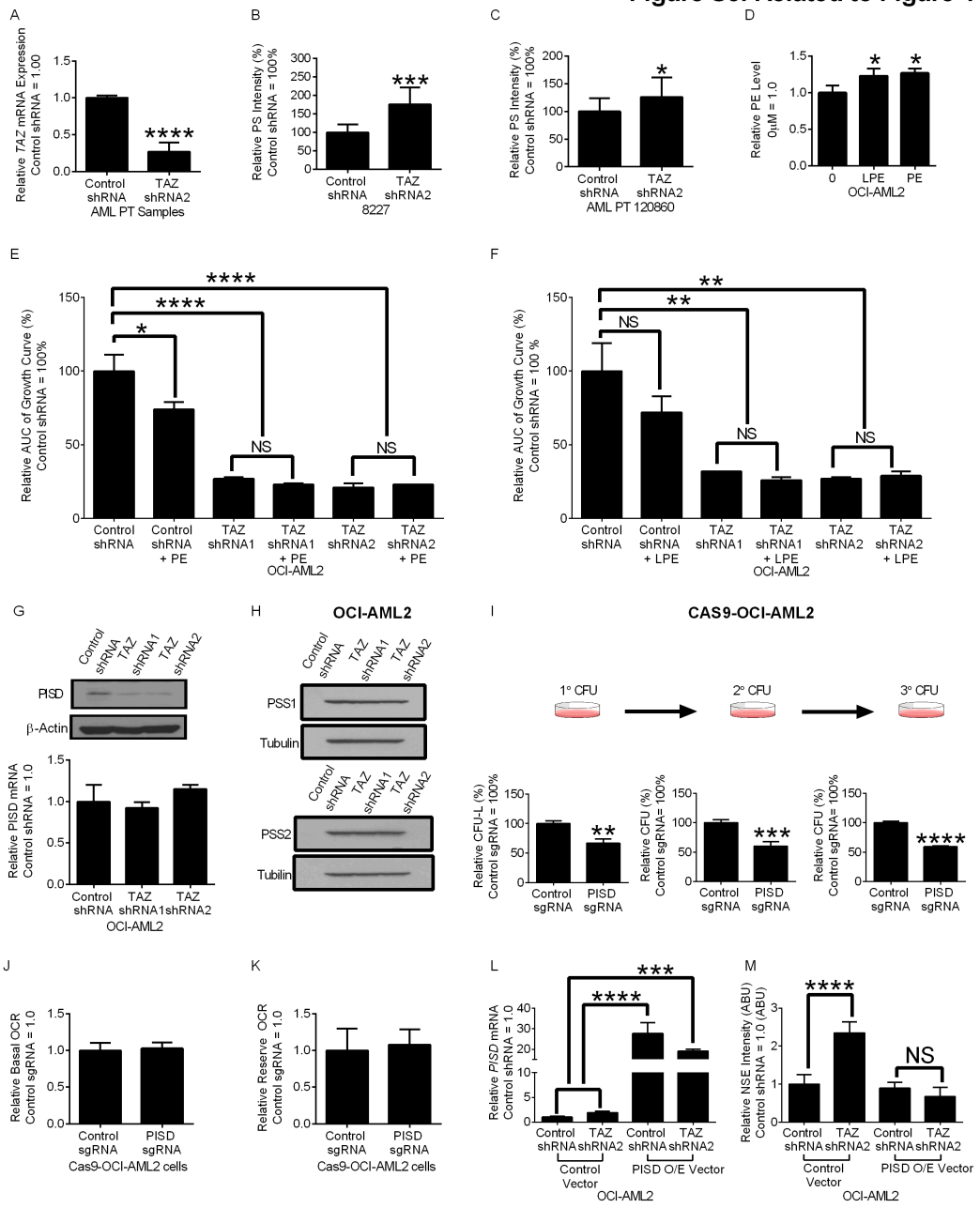

Figure S5. Related to Figure 4 Phosphatidylserine accumulation, as well as PISD decrease is functionally important in AML growth and viability after TAZ-KD.

(A) QRT-PCR of *TAZ* in primary AML cells after TAZ knockdown. Data are mean ± SEM of two independent experiments. ****p≤0.0001 Student's t-test.

(B-C) Intracellular phosphatidylserine levels of 8227 (B), and primary AML cells (C). Data are mean integrated PS staining intensity/DAPI+ cells ± SD (n = 8-12 images). *p≤0.5, ***p≤0.001 by Student's t-test.

(D) Phosphatidylethanolamine (PE) levels in OCI-AML2 cells after PE or lyso-phosphatidylethanolamine (LPE) supplementation. Data are mean ± SD (n = 3, Control = 1.0). *p<0.05 by one-way ANOVA, and Dunnett's post hoc test.

(E-F) Proliferation TAZ knockdown OCI-AML cells after PE (E) or LPE (F) supplementation. The relative area under the curve (AUC) of viable cell counts 12 days after transduction is shown (Control shRNA = 100%). Data represents mean ± SD of representative experiment from 3 independent experiments. *p<0.05, **p≤0.01, ****p≤0.001 by one-way ANOVA and Tukey's post hoc test.

(G) Protein and mRNA levels of the PE synthesizing enzyme phosphatidylserine decarboxylase (PISD) in OCI-AML2 cells after TAZ knockdown. An immunoblot from three independent experiments is shown. QRT-PCR data are mean ± SD (n = 3, Control shRNA=1.0).

(H) Protein levels of the PS synthesizing enzymes PS synthase 1 (PSS1) and PS synthase 2 (PSS2) in OCI-AML2 cells after TAZ knockdown. An immunoblot from four independent experiments is shown.
(I) Clonogenic growth of Cas9-OCI-AML2 after PISD knockout upon serial replating. Data are relative mean ± SEM of 2 independent experiments. (Control sgRNA=100%). **p≤0.01 ***p≤0.001, ****p≤0.001 by Student's t-test.
(J-K) Basal OCR (J) and reserve OCR (K) in of Cas9-OCI-AML2 after PISD knockout. Data are relative mean ± SD of a representative experiment from 2 independent experiments (Control shRNA = 1.0).
(L-M) PISD mRNA expression (L) and NSE staining (M) of TAZ knockdown OCI-AML2 cells after PISD over expression. In (L) Data are mean ± SD (n = 3). ***p≤0.001, ****p≤0.0001 by one-way ANOVA and Tukey's post hoc test. In (M) data represent relative mean ± SD of a representative experiment from 2 independent experiments (Control shRNA = 100%). ****p≤0.0001 by one-way ANOVA and Tukey's post hoc test.

Figure S6. Related to Figure 6

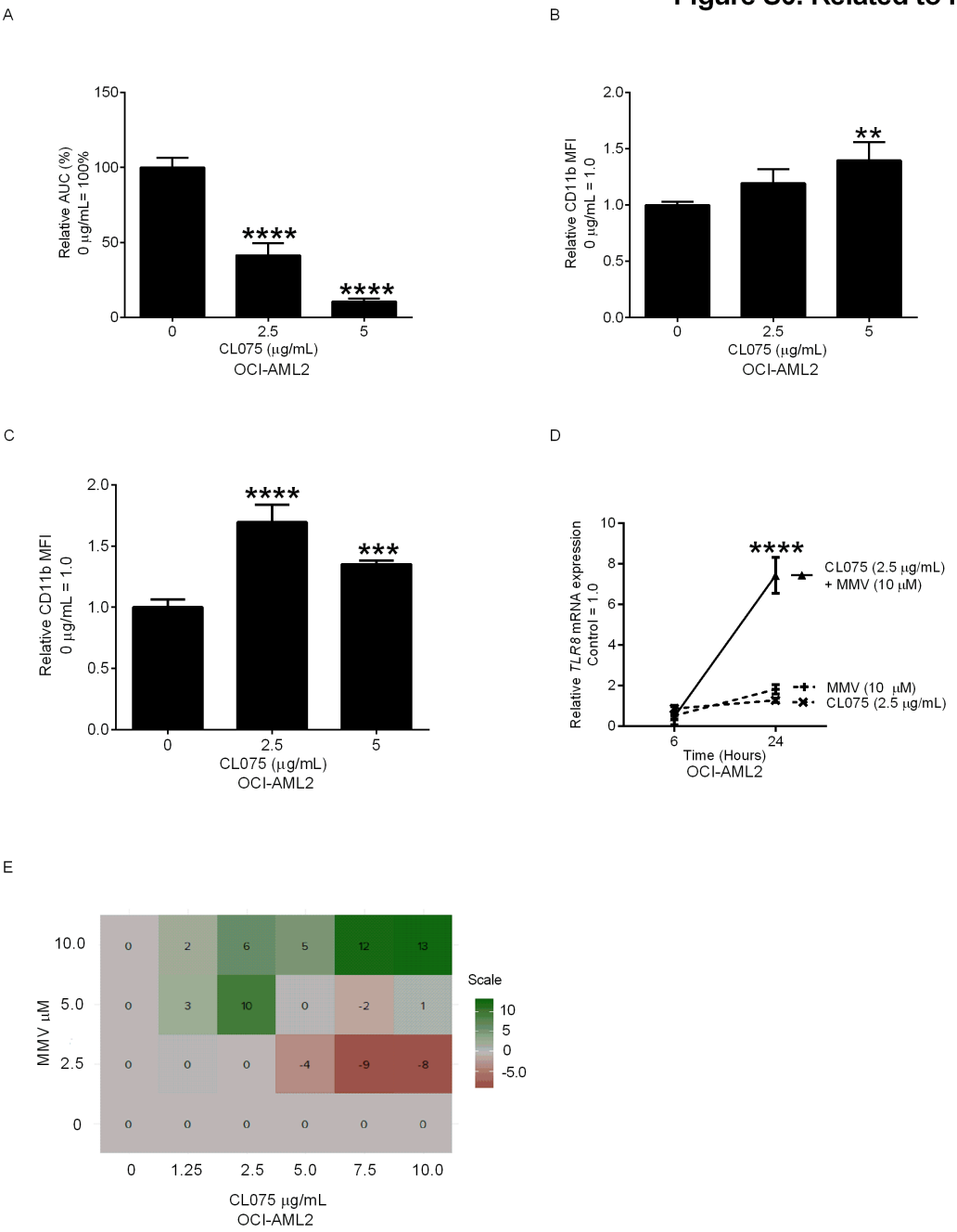

Figure S6. Related to Figure 6. TLR8 agonist CL075 reduces stemness in OCI-AMl2 cells, and synergizes with MMV007285.
(A) Proliferation of OCI-AML2 cells after treatment with increasing concentrations of CL075 or vehicle controls. The relative AUC of viable cell counts over 14 days are shown (Control shRNA = 100%). Data are the relative mean ± SEM (0µM = 100%) of two independent experiments. ***p≤0.001, ****p≤0.0001 by one-way ANOVA and Dunnett's post hoc test.
(B-C) CD11b expression in OCI-AML2 cells seven (B) or fourteen (C) days after treatment with CL075. Data are elative mean fluorescent intensity (MFI) ± SEM of 2-3 independent experiments (0µM = 1.0). **p≤0.01, ***p≤0.001, **** p≤0.0001 by one-way ANOVO and Dunett's post hoc test.
(D) QRT-PCR of toll-like receptor 8 (*TLR8*) of OCI-AML2 cells were treated with 6 or 24 hours after treatment with MMV007285 alone, CL075 alone or MMV007285 + CL075. Data represent mean ± SD (n = 3, Control, 0µM MMV + 0µg/mL CL075 = 1.0). **** p≤0.0001 by Two-Way ANOVA and Tukey's post hoc test.
(E) Excess over bliss additivism score of the combination of MMV007285 and CL075 on cell viability. A representative experiment of two independent experiments is shown.

Figure S7. Related to Figure 7

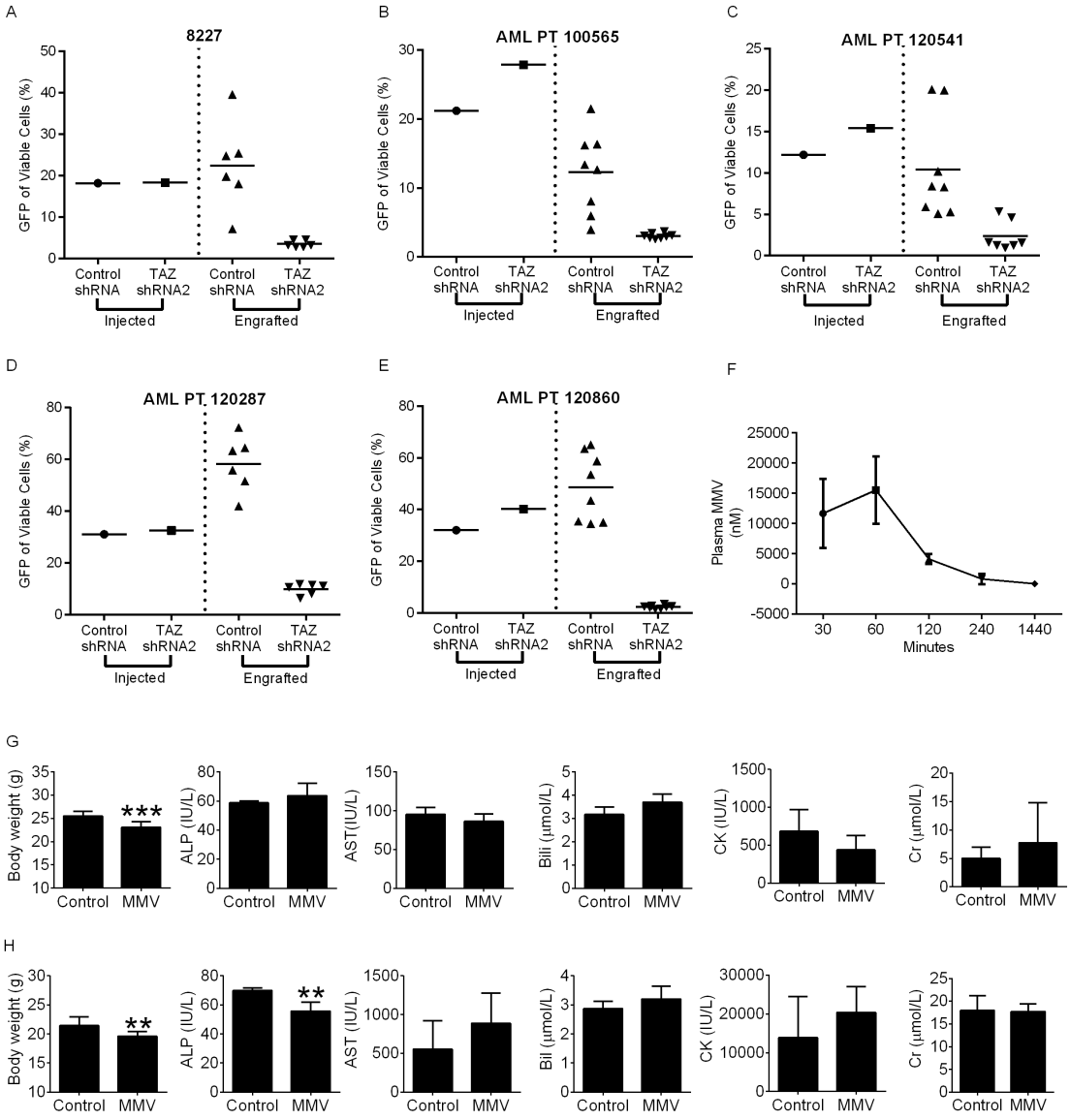

Figure S7. Related to figure 7 increased PS reduces leukemia burden in xenograft models of human AML.
(A-E) Raw data of the engraftment experiment performed in 8227 (A), and AML patient sample cells (B-E) evaluating the impact of TAZ loss on engraftment potential. The y-axis (%GFP+ cells in viable cells) indicates % of shRNA-positive cells in injected or engrafted human cells. In the engrafted group each dot represents an individual mouse, lines represent mean. This figure is related to the normalized relative engraftment potential data presented in Figure 7A-E.
(F) Plasma concentration of intact MM007285 in SCID mice treated with a single dose of MMV007285 (100mg/kg) dissolved in 5% DMSO, 47.5% PEG400, and 47.5% H_20 containing 10% Tween80, via oral gavage. Data represent mean ± SD (n = 3 mice).
(G) Mice body weights, biochemical markers of liver (alkaline phosphatase, aspartate transaminase, bilirubin), muscle (creatine kinase), and renal (creatinine) toxicity of SCID mice xenografted with OCI-AML2 cells MMV007285 or vehicle control. Data represent mean ± SD (n = 10 mice per group for body weights, and n = 4 mice/group for biochemical markers).
(H) Mice body weight, biochemical markers of liver (alkaline phosphatase, aspartate transaminase, bilirubin), muscle (creatine kinase), and renal (creatinine) toxicity of NOD/SCID mice injected with primary AML patient samples treated with MMV007285 or vehicle control. Data represent mean ± SD (n = 9 mice vehicle control group, n=10 mice MMV group). **p<0.01, as determined by Student's t-test

Supplementary Tables

Condition	Mouse Type	Mouse ID	Cell Number (1 x 10^6)
Basal Hematopoiesis	WT	100	58.2
		114	75.9
		115	51.9
		121	39.1
		124	41.8
		130	50.8
		131	44.5
		132	36.7
		133	31.6
		134	31.9
		Average	46.2
		Standard Deviation	12.9
	TAZ-KD	104	50.0
		105	49.2
		108	62.0
		113	57.9
		116	66.0
		122	52.9
		123	53.2
		136	28.3
		Average	52.4
		Standard Deviation	11.4
Hematopoietic Stress (200mg/kg 5-FU)		154	7.2
		156	10.0
		195	22.0
		197	35.0
		198	33.0
		Average	21.4
		Standard Deviation	12.8
	TAZ-KD	152	23.0
		153	12.5
		155	7.1
		159	8.5
		192	19.0
		193	45.0
		Average	19.2
		Standard Deviation	6.82

Table S2.Mouse Bone Marrow Mononuclear Cell Count, Related to Figures 3 and S3.

Cell line	Species	Tissue	Sex	Age
OCI-AML2	*Homo sapiens*, human	Peripheral Blood	Male	65
TEX	*Homo sapiens*, human	Cord Blood	n/a	n/a
U-937	*Homo sapiens*, human	Pleural Effusion	Male	37
K562	*Homo sapiens*, human	Bone Marrow	Female	53
8227	*Homo sapiens,* humans	n/a	n/a	n/a
293T	*Homo sapiens,* humans	Fetal Kidney	n/a	n/a

Table S3. Cell Lines, Related to STAR Methods.

Gene	Strand	Sequence	Reference
***TAZ* (Human AML)**	Forward	5'-TTGCTGCCTTCTGGATTCTT-3'	
	Reverse	5'-CCCTGCCTAAGCTTCTTCCT-3'	This study
***PISD* (Human AML)**	Forward	5'-CAACCTCAGCGAGTTCTTCC-3'	
	Reverse	5'-CGACTCCAGGGAGTAGGTGA-3'	This Study
***18srRNA* (housekeeping, human)**	Forward	5'-AGGAATTGACGGAAGGGCAC-3'	
	Reverse	5'-GGACATCTAAGGGCATCACA-3'	Lab Stock
LYZ	Forward	5'-GCCAAATGGGAGAGTGGTTA-3'	
	Reverse	5'-ATCACGGACAACCCTCTTTG-3'	This Study
iDOX-*Taz*-shRNA Transgene	Forward	5'- CCATGGAATTCGAACGCTGACGTC-3'	
	Reverse	5'- TATGGGCTATGAACTAATGACCC-3'	Khuchua Lab
ND1	Forward	5'-AACATACCCATGGCCAACCT-3'	
	Reverse	5'-AGCGAAGGGTTGTAGTAGCCC-3'	Lab Stock
HGB	Forward	5'-GAAGAGCCAAGGACAGGTAC-3'	
	Reverse	5'-CAACTTCATCCACGTTCACC-3'	Lab Stock
TLR4	Forward	5'-TGAGCAGTCGTGCTGGTATC-3'	
	Reverse	5'-CAGGGCTTTTCTGAGTCGTC-3'	This Study
TLR8	Forward	5'-CAGAGCATCAACCAAAGCAA-3'	
	Reverse	5'-CTGTAACACTGGCTCCAGCA-3'	This Study
IL6	Forward	5'-GGAGACTTGCCTGGTGAAAA-3'	
	Reverse	5'-GTCAGGGGTGGTTATTGCAT-3'	(Murakami et al., 2013)
IFNβ	Forward	5'-CAACTTGCTTGGATTCCTACAAAG-3'	
	Reverse	5'-TATTCAAGCCTCCCATTCAATTG-3'	This Study

Table S4. PCR Primers, Related to STAR Methods.

Patient ID	Disease	Age at Collection	Sex	Cytogenetics	Molecular	Status of Sample
110839	AML, undifferentiated	86	M	58-59,CYY,-2,-3,-4,-5,-6,-7,-9,-12,-13,add(15)(q24)x2,-16,-16,-17,-17,-19,-20,+22,+r,+2-7mar[cp14]	Not Done	Diagnostic
0676	AML, undifferentiated	79	M	46~48,XY,+6,del(13)(q12q22),+del(13)(q12q22)[cp9]/46,XY[11]	Not Done	Diagnostic
120021	AML, with maturation	88	F	46,XX,1~5dmin[13]/46,XX[7	Not Done	Diagnostic
160556	AML with myelodysplasia-related features	57		46,XY,t(3;5)(q21;q35)[10]	Not Done	Diagnostic
162111	AML with mutated NPM1	18	M	45,X,-Y[9]/46,XY[11]	NPM1+, FLT3-ITD-	Diagnostic
100565	AML	65	M	46,XY,t(6;11)(q27;q23)[19]/46,XY[1].nucish(MLLx2)(5'MLLsep 3'MLLx1)[148/200]	Not Done	Diagnostic
120541	AML with mutated NPM1	51	F	46,XX[20]	NPM1+, FLt3-ITD+	Diagnostic
120287	AML with mutated NPM1	77	M	46,XY[20]	NPM1+, FLt3-ITD+	Diagnostic
120860	AML with t(9;11)(p22;q23); MLLT-MLL	31	F	46,XX,t(9;11)(p22;q23)[10]	Not Done	Diagnostic

Table S5. Clinical Characteristics of Primary AML Patient Samples, Related to STAR Methods.

Gene shRNA name	Reference	Sequence
Control sgRNA	N/A	5'-CCCGAATCTCTATCGTGCGG-3'
TAZ sgRNA1	Gene ID: 6901	5'-TACGAGCTCATCGAGAAGCG-3'
TAZ sgRNA2	Gene ID: 6901	5'-GCTCATCGAGAAGCGAGGCC-3'
PISD sgRNA	Gene ID: 23761	5'-AGCTGCCACACTGGCTGCGC-3'
Control shRNA (pLKO.1)	clonetechGfp_587s1c1	5'-CCGG TGC CCG ACA ACC ACT ACC TGA CTCGAG TCA GGT AGT GGT TGT CGG GCA TTTTT-3'
TAZ shRNA1 (pLKO.1)	NM_000116	5'-CCGG TCC TAA CAG TCC GCC CTA CTT CTCGAG AAG TAG GGC GGA CTG TTA GGA TTTTTG-3'
TAZ shRNA2 (pLKO.1)	NM_000116	5'-CCGG TGC TTC CTC AGT TAC ACA AAG CTCGAG CTT TGT GTA ACT GAG GAA GCA TTTTTG-3'
Control shRNA (pRS19)	(Chan et al., 2015)	5'- ACCG GCA CTA CCA GAG CTA ACT CAG ATA GTA CT TCAAGAG AGTA CTA TCT GAG TTA GCT CTG GTA GTGC TTTT-3'
TAZ shRNA2 (pRS19)	NM_000116	5'-ACCG TGC TTC CTC AGT TAC ACA AAG TCAAGAG CTT TGT GTA ACT GAG GAA GCA TTTT -3'

Table S6. sgRNA or shRNA Sequences, Related to STAR Methods.

Lipids	Polarity	Molecular Ion	Mode	m/z ion	NCE	Approximate RT (min)
52:2 MLCL	-	[M-H]-	Top-5 DDA	1165.7666	17.5	11.55 - 11.88
52:3 MLCL	-	[M-H]-	Top-5 DDA	1163.7509	17.5	10.85 - 10.96
52:4 MLCL	-	[M-H]-	Top-5 DDA	1161.7353	17.5	8.79 - 9.53
54:2 MLCL	-	[M-H]-	Top-5 DDA	1193.7979	17.5	12.46 - 12.76
54:3 MLCL	-	[M-H]-	Top-5 DDA	1191.7822	17.5	11.45 - 11.90
54:4 MLCL	-	[M-H]-	Top-5 DDA	1189.7666	17.5	10.41 - 10.90
54:5 MLCL	-	[M-H]-	Top-5 DDA	1187.7509	17.5	9.26 - 9.71
54:6 MLCL	-	[M-H]-	Top-5 DDA	1185.7353	17.5	10.32 - 10.66
64:3 CL	-	[M-H]-	Top-5 DDA	1345.9188	17.5	14.51 - 14.74
66:2 CL	-	[M-H]-	Top-5 DDA	1375.9659	17.5	16.29 - 16.45
66:3 CL	-	[M-H]-	Top-5 DDA	1373.9502	17.5	15.41 - 15.70
66:4 CL	-	[M-H]-	Top-5 DDA	1371.9345	17.5	14.57 - 14.85
68:3 CL	-	[M-H]-	Top-5 DDA	1401.9816	17.5	16.23 - 16.55
68:4 CL	-	[M-H]-	Top-5 DDA	1399.9659	17.5	15.42 - 15.76
68:5 CL	-	[M-H]-	Top-5 DDA	1397.9493	17.5	14.71 - 14.98
70:4 CL	-	[M-H]-	Top-5 DDA	1427.9973	17.5	16.21 - 16.55
70:5 CL	-	[M-H]-	Top-5 DDA	1425.9817	17.5	15.54 - 15.85
70:6 CL	-	[M-H]-	Top-5 DDA	1423.9660	17.5	14.85 - 15.20
70:7 CL	-	[M-H]-	Top-5 DDA	1421.9503	17.5	15.43 - 15.73
72:5 CL	-	[M-H]-	Top-5 DDA	1454.0131	17.5	16.40 - 16.59
72:6 CL	-	[M-H]-	Top-5 DDA	1451.9974	17.5	15.69 - 15.97
72:7 CL	-	[M-H]-	Top-5 DDA	1449.9817	17.5	16.24 - 16.54
72:8 CL	-	[M-H]-	Top-5 DDA	1447.9661	17.5	15.55 - 15.81
72:9 CL	-	[M-H]-	Top-5 DDA	1445.9504	17.5	14.87 - 15.07
74:6 CL	-	[M-H]-	Top-5 DDA	1480.0288	17.5	16.52 - 16.59
74:7 CL	-	[M-H]-	Top-5 DDA	1478.0131	17.5	15.91 - 16.08
74:8 CL	-	[M-H]-	Top-5 DDA	1475.9975	17.5	16.36 - 16.61
74:9 CL	-	[M-H]-	Top-5 DDA	1473.9818	17.5	15.72 - 15.94

Table S7. Detection of Lipids by MS/MS, Related to STAR Methods. Abbreviations: MLCL = mono-lyso cardiolipin, CL – cardiolipin, DDA = data-dependent acquisition, m/z = mass-to-charge ratio, NCE = normalized collision energy, RT = retention time